WEAR MODE TRANSITION DURING THE MICRO-SCALE ABRASION OF WC-Co P20 AND M2 TOOL STEEL

Ronaldo Câmara Cozza
Surface Phenomena Laboratory, Department of Mechanical Engineering, Polytechnic School, University of São Paulo, Av. Prof. Mello Moraes 2231, São Paulo, SP 05508-900, Brazil
ronaldo.cozza@poli.usp.br

Roberto Martins Souza
Surface Phenomena Laboratory, Department of Mechanical Engineering, Polytechnic School, University of São Paulo, Av. Prof. Mello Moraes 2231, São Paulo, SP 05508-900, Brazil
roberto.souza@poli.usp.br

Deniol Katsuki Tanaka
Surface Phenomena Laboratory, Department of Mechanical Engineering, Polytechnic School, University of São Paulo, Av. Prof. Mello Moraes 2231, São Paulo, SP 05508-900, Brazil
dktanaka@usp.br

Abstract. *This work presents a study on the phenomena that occur during micro-scale abrasion (ball cratering) tests. In particular, a fixed-sphere equipment was used to evaluate the transition from three-body (rolling abrasion) to two-body (grooving abrasion) abrasion modes. The transition was studied for different combinations of ball and specimen materials. Ball materials were cemented AISI 1010 steel and, as testing specimen materials, WC-Co P20 and M2 steel tool were used. An abrasive slurry, prepared with black silicon carbide (SiC) particles (average particle size of 5μm), was supplied to the contact between the specimen and the ball. The wear craters were later examined under an optical microscope, in order to evaluate wear mode transition as a function of the applied load and the slurry concentration. Mixed-mode abrasion (two-body abrasive wear + three-body abrasive wear) was observed in the tests with M2 tool steel. For the WC-Co P20 specimen, both grooving abrasion and mixed-mode abrasion were observed, depending on the test condition. All results are in qualitative agreement with those found in the literature.*

Keywords: *Two-body abrasive wear, three-body abrasive wear, micro-abrasive wear test.*

1. Introduction

According to Hutchings (1998), there are two modes of abrasive wear: two-body abrasive wear ("*grooving abrasion*") and three-body abrasive wear ("*rolling abrasion*"). Considering two surfaces in relative movement, in the two-body abrasive wear, the abrasive particles are fixed to one of the surfaces. Consequently, the particles can only slide over the counter-body. In the three-body abrasive wear, the abrasive particles are free, and then, the particles can roll between the surfaces. It is possible, in this case, to have some degree of sliding, but with minor intensity. Considering the two forms of movement, under identical conditions of test, the two-body abrasive mode provides higher wear rates than the three-body abrasive wear.

With a micro-abrasive testing machine with fixed ball, it is possible to study the abrasive wear of materials under many test conditions. Figure 1 shows the principle of this equipment.

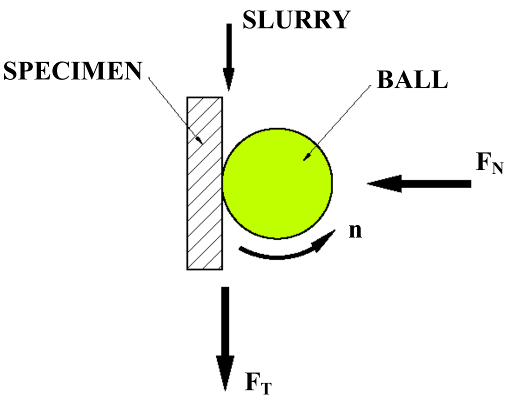

Figure 1. Principle of operation of the micro-abrasive wear testing machine.

A normal force (F_N) is responsible for the contact between the ball and the specimen. The contact and the relative movement between these two elements generate a tangencial force (friction force), F_T. The fixed sphere configuration allows wider ranges of normal loads, when compared with those of the free ball configuration (Gee *et al.*, 2005).

The works of Trezona, Allsopp and Hutchings (1999), Trezona and Hutchings (1999), Adachi and Hutchings (2003), Adachi and Hutchings (2005) and Mergler and Huis in 't Veld (2003) showed that changes in the value of normal force, slurry concentration, hardness, shape and size of abrasive particles and ball and specimen materials can, during the micro-abrasive wear test, modify the wear mode, from three-body abrasive wear to two-body abrasive wear. During this transition, it is possible to obtain conditions where both modes occur simultaneously.

The objective of this work is to study this wear mode transition, by variation of test conditions and materials (ball and specimen) used.

2. Materials and Methods

2.1. Micro-abrasion wear testing machine

The Micro-Abrasion Wear Testing Machine - Model LFS 2005 performs abrasive wear tests, and allows the evaluation of the wear behavior of metallic and non-metallic materials. Figure 2 presents a global view of the equipment.

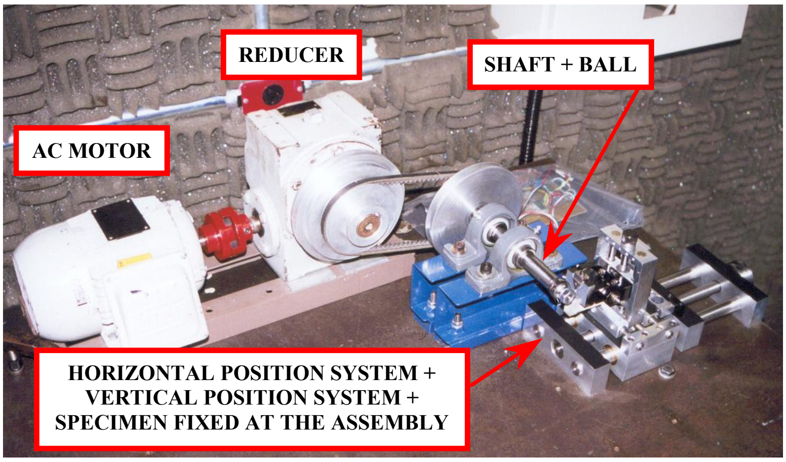

Figure 2. Global view of the Micro-Abrasion Wear Testing Machine - Model LFS 2005.

Through an AC motor, reducer and a frequency inventer, it is possible to obtain a range of rotations of the ball, from 0 to 525 rpm. Figure 3 shows the principal translation system. Part B is responsable for the translation movement of the specimen, which is forced against the ball. Between parts A and B there is a load cell (C), that reads the normal force developed during the test. The normal force is applied by the rotation of the fusee (D).

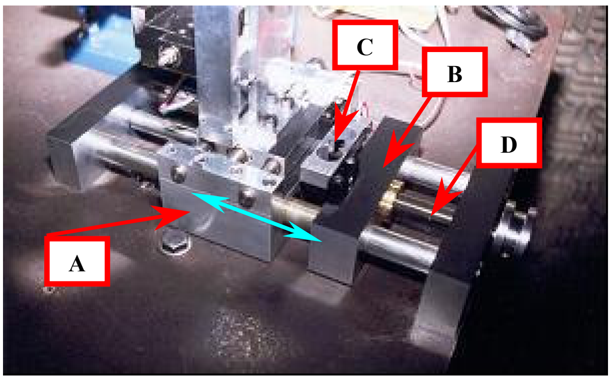

Figure 3. Detail of the assembly responsible for the application of the normal load.

Many experiments may be conducted in a single specimen. The equipment has a horizontal positioning system (HPS) and a vertical positioning system (VPS). The specimen position, for both systems, may be adjusted with a precision of 10μm. Both systems are fixed to element A (Fig. 3).

Assembled to the VPS is the specimen holder (Fig. 4). The mechanism shown in this figure only allows the mounting of triangular specimen (equilateral triangle with 16 mm edges), or the use WC-Co triangular inserts with geometry similar to ISO TPGN 160308. During the tests, the abrasive slurry was supplied between the ball and the specimen by a seringe.

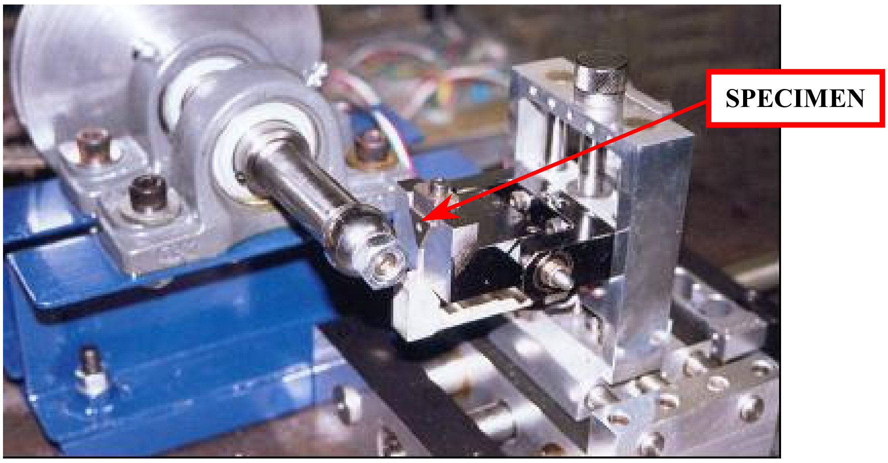

Figure 4. WC-Co interchange pastille fixed at the assembly.

2.2. Materials

Specimen materials were WC-Co P20 and M2 tool steel. Ball materials were cemented AISI 1010 steel, with diameter of 25,40 mm. The abrasive slurry was manufactured with commercial black silicon carbide SiC 1000, from Alcoa. Figure 5 (Izhevskyi *et al.*, 2004) presents a scanning electron micrograph of the abrasive used in this work.

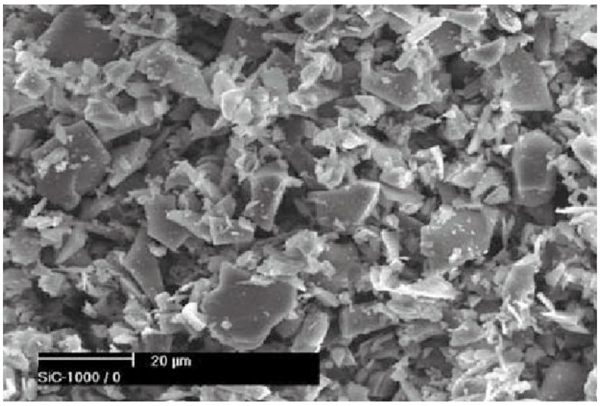

Figure 5. Result of SEM examination of SiC 1000 (Izhevskyi *et al.*, 2004).

The particle size distribution of this material is shown in Fig. 6 (Izhevskyi *et al.*, 2004).

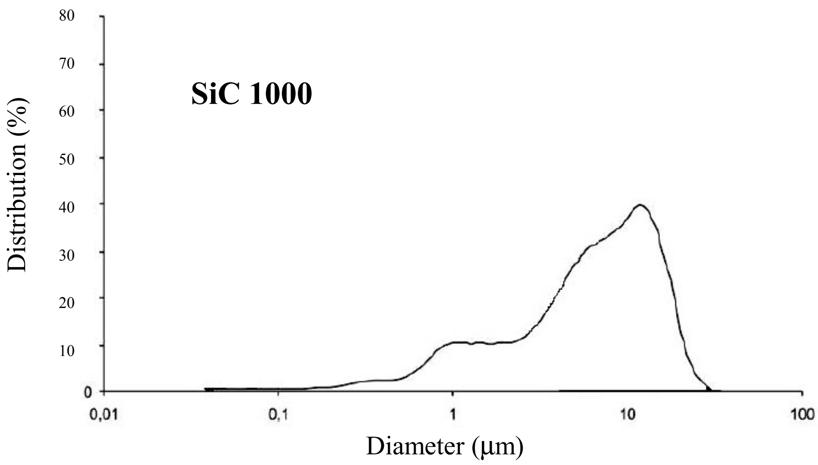

Figure 6. Particle size distribution of SiC 1000 (Izhevskyi *et al.*, 2004).

Table 1 shows the hardness of the materials used for specimens, balls and abrasive particles.

Table 1. Hardness of materials used for specimens and abrasive particles.

	Material	Hardness (GPa)
Specimen	M2 steel tool	8 - 9
	WC-Co P20	15
Ball	Cemented AISI 1010 steel	8 - 8,5[(1)]
Abrasive particle	SiC	18,5 - 19

[(1)]: At surface

2.3. Experimental procedure

Each specimen was tested at conditions 1 and 2, defined in Tab. 2, to provide a total of 4 experimental conditions. All the tests were conducted without intermediate stops. Four repetitions were conducted for each test condition.

Table 2. Values of parameters established for the tests.

Test Condition	1	2
Normal Force (N)	1,25	5
Rotation of ball (rpm)	15	
Time of test (min)	5	

The slurry concentration was defined as indicated in Tab. 3. The two columns on the left show the percentage, in volume, of SiC and distiled water. The column on the right provides the mass of SiC per unit volume of distiled water ($g_{SiC}/cm^3_{Dist.\ Water}$).

Table 3. Slurry concentration.

% SiC (VOLUME)	% Distiled Water (VOLUME)	$\frac{g_{SiC}}{cm^3 H_2O - Dist.}$
25	75	1,045

The sliding speed of the ball was defined based on the literature (Trezona, Allsopp and Hutchings, 1999) and considering the hardness of the specimen and the ball. The normal forces and the slurry concentration were also established based on the literature (Trezona, Allsopp and Hutchings, 1999).

3. Results and discussion

All the tests conducted on the M2 tool steel resulted in mixed-mode abrasion. On the other hand, in the tests on the WC-Co P20 specimen it was not possible to observe the full predominancy of three-body abrasive wear. The two-body abrasive wear was observed in a high normal force, 5 N. At a low load, 1,25 N, the mixed-mode abrasion was present. In this case, in the centre of scar, two-body abrasive wear was seen and, at the edges, three-body abrasive wear occurred (Fig. 7). Adachi and Hutchings (2003) observed the same behaviour, but the specimen materials were of PMMA (poly methyl methacrylate).

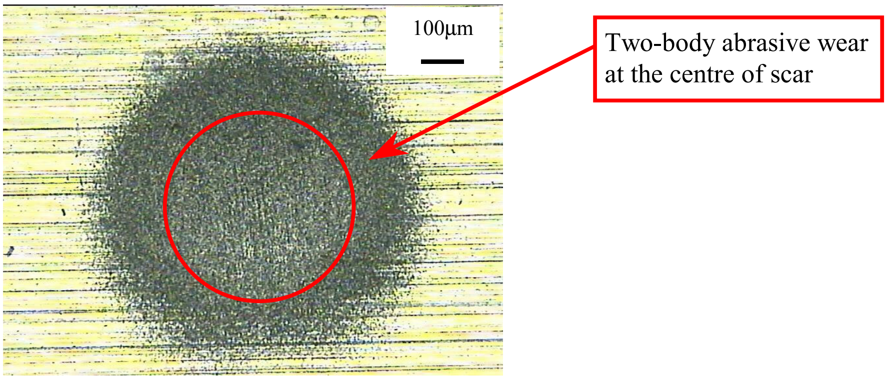

Figure 7. Action of two-body abrasive wear (centre) and three-body abrasive wear (edges), for a normal force of 1,25 N and a slurry concentration of 1,045 g/cm^3 (25% SiC / 75% distilated water).

In each specimen, for each condition, all the scars were similar. However, for the normal force of 5 N, the fourth repetition resulted in a small difference in the shape of the wear crater, when compared with the other three. Figure 8 shows the shape of the wear crater obtained after the fourth repetition of a test condition with M2 tool steel specimens.

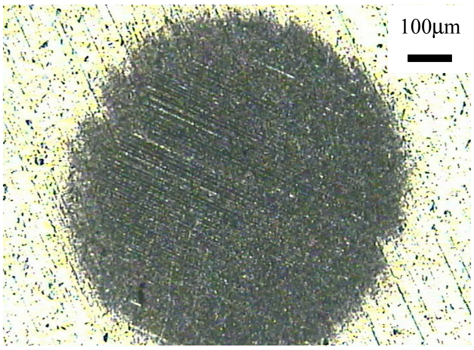

Figure 8. Wear crater in a M2 tool steel apecimen, for a normal force of 5 N and a slurry concentration of 1,045g/cm^3 (25% SiC / 75% distilated water). This wear crater was the fourth test conducted on the specimen.

Trezona, Allsopp and Hutchings (1999) mention that, for high slurry concentrations and low normal forces, the three-body abrasive wear predominates and, for high normal forces and low slurry concentrations, the two-body abrasive wear domiates. In this work, a similar behaviour was observed. For the normal force of 1,25 N, mixed-mode abrasion occured. However, for the normal force of 5 N (relatively high when compared with 1,25 N) two-body abrasive wear was observed at the WC-Po P20 specimen. Figure 9 reproduces a result originally published by Adachi and Hutchings (2003), onto which the results obtained in this work were superimposed.

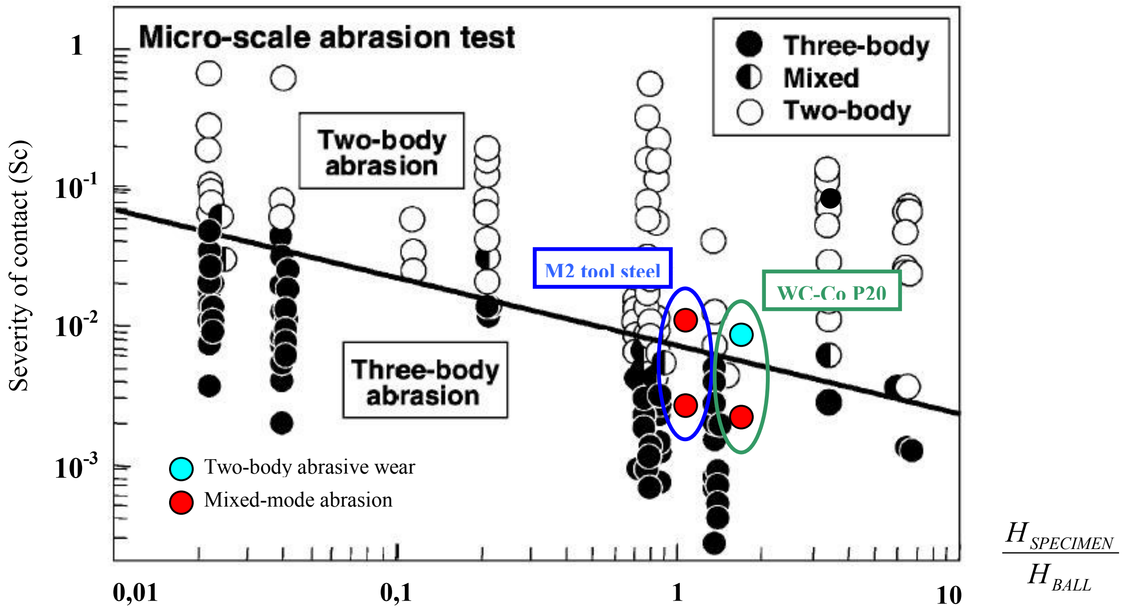

Figure 9. Graphic exhibiting the actuation of two-body abrasive wear and mixed-mode abrasion.

The severity of contact (Sc), may be expressed as (Adachi and Hutchings, 2003; Hutchings, 1998):

$$S_C = \frac{F_N\left(\dfrac{1}{H_{BALL}}+\dfrac{1}{H_{SPEC}}\right)}{\pi\left[\sqrt[3]{\left[0{,}75.F_N.R\left(\dfrac{1-\nu_{BALL}^2}{E_{BALL}}+\dfrac{1-\nu_{SPEC}^2}{E_{SPEC}}\right)\right]^2}+2.R.D_P\right]\vartheta} \qquad (1)$$

where F_N is the normal force, R is the radius of the sphere, D_P is the average particle size of abrasive particles and ϑ is the volume fraction of abrasive in the slurry.

The results obtained are in qualitative agreement with the works presented by Adachi and Hutchings (2003) and Trezona, Allsopp and Hutchings (1999), with respect to the wear mode transition during the micro-scale abrasion. In both cases, two-body abrasive wear was favored when the severity of contact (Sc) was increased. However, it is important to mention that Sc does not consider some important parameters of the micro-scale abrasion test, such as abrasive hardness, shape and particle size. The results obtained in this work does not provide evidence to the use of the map by Adachi and Hutchings (2003) to other types of abrasive particles, since the abrasive used in this work was similar to the one used by Adachi and Hutchings (2003).

Furthermore, it is also important to mention that during a micro-abrasive wear test, specimen and ball are never in contact. Between these two elements there are abrasive particles, that generate the two-body abrasive wear or the three-body abrasive wear or mixed-mode abrasion at the specimen, depending on the test parameters. However, this fact is not considered by some authors, for example, Adachi and Hutchings in their works (2003; 2005).

4. Conclusions

The ball material was a limiting factor during the tests. Cemented AISI 1010 steel was not a good material for these tests. The small deviations from circularity, observed during the fourth repetition of certain test conditions, may be an indication of ball wear. In the case of a cemented ball, this wear probably results in a decrease in surface hardness throughout the tests, which may introduce experimental artifacts.

The four points superimposed in the Fig. 9 show that the results obtained in this work are in qualitative agreement with the results obtained by Adachi and Hutchings (2003). Further research is still necessary to verify these agreement in other test conditions, including those with different abrasive materials.

5. Acknowledgements

For the Mr. José Carlos Cavale - FEROSÃO J. C. R. Ind. Com. Ltda. (ferosão@ferosão.com.br / (11) 4352-5600) by M2 tool steel specimen.

For the Prof. Dr. José Carlos Bressiani, by SiC.

For the friend Raquel Camponucci, by help with the optical microscope images.

6. References

Adachi, K., Hutchings, I. M., 2003, “Wear-mode mapping for the micro-scale abrasion test”, Wear, Vol. 255, pp. 23-29.

Adachi, K., Hutchings, I. M., 2005, “Sensitivity of wear rates in the micro-scale abrasion test to test conditions and material hardness”, Wear, Vol. 258, pp. 318-321.

Gee, M. G., Gant, A. J., Hutchings, I. M., Kusano, Y., Schiffman, K., Van Acker, K., Poulat, S., Gachon, Y., von Stebut, J., Hatto, P., Plint, G., 2005, “Results from an interlaboratory exercise to validate the micro-scale abrasion test”, Wear, Vol. 259, pp. 27-35.

Hutchings, I. M., 1998, “Tribology - Friction and Wear of Engineering Materials”, 7ª. edição, Ed. Edward Arnold, London, England, 273 p.

Izhevskyi, V. A., Genova, L. A., Bressiani, J. C., Bressiani, A. H. A., 2004, “Liquid phase sintered SiC ceramics from starting materials of different grade”, Cerâmica, Vol. 50, pp. 261-267.

Mergler, Y. J., Huis in ‘t Veld, A. J., 2003, “Micro-abrasive wear of semi-crystalline polymers”, Tribological Research and Design for Engineering Systems, pp. 165-173.

Trezona, R. I., Allsopp, D. N., Hutchings, I. M., 1999, “Transitions between two-body and three-body abrasive wear: influence of test conditions in the microscale abrasive wear test”, Wear, Vol. 225-229, pp. 205-214.

Trezona, R. I., Hutchings, I. M., 1999, “Three-body abrasive wear testing of soft materials”, Wear, Vol. 233-235, pp. 209-221.

7. Responsibility notice

The authors are the only responsible for the printed material included in this paper.